Te   Report S   on the
B   osystem-A   sphere Study (BOREAS)

ll and Jaime Nickeson, Editors

52

S RSS-7 Regional LAI and FPAR Images
R-LAC Composites

J. Cihlar

nautics and
stration

ce Flight Center
yland 20771

Aug

The NASA STI Program Office ... in Profile

Since its founding, NASA has been dedicated to the advancement of aeronautics and space science. The NASA Scientific and Technical Information (STI) Program Office plays a key part in helping NASA maintain this important role.

The NASA STI Program Office is operated by Langley Research Center, the lead center for NASA's scientific and technical information. The NASA STI Program Office provides access to the NASA STI Database, the largest collection of aeronautical and space science STI in the world. The Program Office is also NASA's institutional mechanism for disseminating the results of its research and development activities. These results are published by NASA in the NASA STI Report Series, which includes the following report types:

- TECHNICAL PUBLICATION. Reports of completed research or a major significant phase of research that present the results of NASA programs and include extensive data or theoretical analysis. Includes compilations of significant scientific and technical data and information deemed to be of continuing reference value. NASA's counterpart of peer-reviewed formal professional papers but has less stringent limitations on manuscript length and extent of graphic presentations.

- TECHNICAL MEMORANDUM. Scientific and technical findings that are preliminary or of specialized interest, e.g., quick release reports, working papers, and bibliographies that contain minimal annotation. Does not contain extensive analysis.

- CONTRACTOR REPORT. Scientific and technical findings by NASA-sponsored contractors and grantees.

- CONFERENCE PUBLICATION. Collected papers from scientific and technical conferences, symposia, seminars, or other meetings sponsored or cosponsored by NASA.

- SPECIAL PUBLICATION. Scientific, technical, or historical information from NASA programs, projects, and mission, often concerned with subjects having substantial public interest.

- TECHNICAL TRANSLATION. English-language translations of foreign scientific and technical material pertinent to NASA's mission.

Specialized services that complement the STI Program Office's diverse offerings include creating custom thesauri, building customized databases, organizing and publishing research results . . . even providing videos.

For more information about the NASA STI Program Office, see the following:

- Access the NASA STI Program Home Page at http://www.sti.nasa.gov/STI-homepage.html

- E-mail your question via the Internet to help@sti.nasa.gov

- Fax your question to the NASA Access Help Desk at (301) 621-0134

- Telephone the NASA Access Help Desk at (301) 621-0390

- Write to:
  NASA Access Help Desk
  NASA Center for AeroSpace Information
  7121 Standard Drive
  Hanover, MD 21076-1320

NASA/TM—2000–209891, Vol. 52
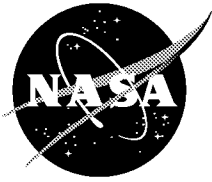
Technical Report Series on the
Boreal Ecosystem-Atmosphere Study (BOREAS)

Forrest G. Hall and Jaime Nickeson, Editors

Volume 52

BOREAS RSS-7 Regional LAI and FPAR Images
From 10-Day AVHRR-LAC Composites

Jing Chen and Josef Cihlar
Canada Centre for Remote Sensing, Ottawa, Ontario, Canada

August 2000

Available from:

BOREAS RSS-7 Regional LAI and FPAR Images From Ten-Day AVHRR-LAC Composites

Jing M. Chen, Josef Cihlar

Summary

The BOREAS RSS-7 team collected various data sets to develop and validate an algorithm to allow the retrieval of the spatial distribution of LAI from remotely sensed images. AVHRR level-4c 10-day composite NDVI images produced at CCRS were used to produce images of LAI and the FPAR absorbed by plant canopies for the three summer IFCs in 1994 across the BOREAS region. The algorithms were developed based on ground measurements and Landsat TM images (Chen and Cihlar, 1996; Chen, 1996b). The data are stored in binary image format files.

Note that some of the data files on the BOREAS CD-ROMs have been compressed using the Gzip program. See Section 8.2 for details.

Table of Contents

1. Data Set Overview

1.1 Data Set Identification
BOREAS RSS-07 Regional LAI and FPAR Images From Ten-Day AVHRR-LAC Composites

1.2 Data Set Introduction
These Leaf Area Index (LAI) and Fraction of Photosynthetically Active Radiation (FPAR) images were generated in response to the need within the BOReal Ecosystem-Atmosphere Study (BOREAS) modeling community for adequate spatial and temporal coverage of LAI and FPAR estimates across the BOREAS region. The 10-Day Advanced Very High Resolution Radiometer (AVHRR) composite Normalized Difference Vegetation Index (NDVI) images, produced after various processing steps to remove artifacts, are very suitable for this purpose. Although algorithms for some cover types for this region are not available, these parameter maps were produced as the best estimates at this stage.

1.3 Objective/Purpose

The objective of this project was to provide quantitative spatial distribution of LAI and FPAR for the BOREAS region for the 1994 summer Intensive Field Campaigns (IFCs) for the purpose of modeling the carbon, water, energy, and trace gas exchange between the boreal ecosystems and the atmosphere.

1.4 Summary of Parameters

LAI and FPAR absorbed by plant canopies.

1.5 Discussion

These LAI and FPAR images are based on AVHRR level-4c NDVI products and a coregistered land cover map (Pokrant, 1991). The level-4c product is based on the AVHRR level-4b product, but is further processed to remove or mitigate some artifacts caused by the input data or the compositing process. The artifacts of concern are atmospheric contamination and bidirectional reflectance effects for AVHRR channels 1 and 2, and atmospheric and surface emissivity effects for AVHRR channel 4. The processing was carried out at the Canadian Centre for Remote Sensing (CCRS) using software and procedures developed in-house (see Section 9 for details). The spatial and temporal coverage of this product is identical to that of the level-4b and -4c products.

1.6 Related Data Sets

BOREAS RSS-07 LAI, Gap Fraction, and FPAR Data
BOREAS Level-4c AVHRR-LAC Ten-Day Composite Images: Surface Parameters
BOREAS Level-4b AVHRR-LAC Ten-Day Composite Images: At-sensor Radiance

2. Investigator(s)

2.1 Investigator(s) Name and Title

Dr. Jing M. Chen
Dr. Josef Cihlar

2.2 Title of Investigation

Retrieval of Boreal Forest Leaf Area Index From Multiple Scale Remotely Sensed Vegetation Indices

2.3 Contact Information

Contact 1:
Jing M. Chen
Canada Centre for Remote Sensing
588 Booth Street, 4th Floor
Ottawa, Ontario
K1A0Y7 Canada
(613) 947-1266
(613) 947-1406 (fax)
jing.chen@ccrs.nrcan.gc.ca

Contact 2:
Josef Cihlar
Canada Centre for Remote Sensing
588 Booth Street, 4th Floor
Ottawa, Ontario
K1A0Y7 Canada
(613) 947-1265
(613) 947-1406 (fax)
Josef.Cihlar@ccrs.nrcan.gc.ca

Contact 3:
Jaime Nickeson
Raytheon ITSS
NASA GSFC
Code 923
Greenbelt, MD 20771
(301) 286-3373
Jaime.Nickeson@gsfc.nasa.gov

3. Theory of Measurements

The theories of LAI and FPAR measurements are documented in the Remote Sensing Science (RSS)-07 ground LAI and FPAR data document. The theory of AVHRR measurements is given in the BOREAS level-4c AVHRR images document, but the relevant portions are copied below.

The AVHRR is a four- or five-channel scanning radiometer capable of providing global daytime and nighttime information about ice, snow, vegetation, clouds, and the sea surface. These data are obtained on a daily basis primarily for use in weather analysis and forecasting; however, a variety of other applications are possible. The AVHRR-Local Area Coverage (LAC) data collected for the BOREAS project were from instruments onboard National Oceanic and Atmospheric Administration (NOAA)-9, NOAA-11, and NOAA-12 polar orbiting platforms. The radiometers measured emitted and reflected radiation in the visible, near-infrared, one middle-infrared, and one or two thermal channels.

The primary use of each channel and spectral regions and bandwidths on the respective NOAA platforms are given in the following tables:

Channel	Wavelength [micrometers]	Primary Use
1*	0.57 - 0.69	Cloud and Surface Mapping
2	0.72 - 0.98	Surface Water Delineation, Vegetation Cover
3	3.52 - 3.95	Sea Surface Temperature (SST), Nighttime Cloud Mapping
4**	10.3 - 11.4	Surface Temperature, Day/Night Cloud Mapping
5***	11.4 - 12.4	Surface Temperature

* Channel 1 wavelength for the Television and Infrared Observation Satellite (TIROS)-N flight model was 0.5 -0.90 micrometers.
** For NOAA-7 and-9, channel 4 was 10.3-11.3 micrometers.
*** For TIROS-N, NOAA-6, -8, -10, and-12 Channel 5 duplicates Channel 4.

The wavelength ranges at 50% relative spectral response (in micrometers) of the bands for the platform-specific instruments are:

```
Band       NOAA-9           NOAA-11          NOAA-12          NOAA-14
----    ---------------   ---------------  ---------------   ---------------
 1       0.570 -  0.699    0.572 -  0.698   0.571 -  0.684    0.570 -  0.699
 2       0.714 -  0.983    0.716 -  0.985   0.724 -  0.984    0.714 -  0.983
 3       3.525 -  3.931    3.536 -  3.935   3.554 -  3.950    3.525 -  3.931
 4      10.334 - 11.252   10.338 - 11.287  10.601 - 11.445   10.330 - 11.250
 5      11.395 - 12.342   11.408 - 12.386  10.601 - 11.445   11.390 - 12.340
```

The AVHRR is capable of operating in both real-time and recorded modes. Direct readout data were transmitted to ground stations of the automatic picture transmission (APT) class at low resolution (4 x 4 km) and to ground stations of the high-resolution picture transmission (HRPT) class at high resolution (1 x 1 km). AVHRR HRPT data were received for the BOREAS region by the CCRS Prince Albert Satellite Station (PASS). The LAI and FPAR images in 1994 in this data set were produced using the NOAA-11 sensor.

4. Equipment

4.1 Sensor/Instrument Description

The AVHRR is a cross-track scanning system featuring one visible, one near-infrared, one middle-infrared, and two thermal channels. The analog data output from the sensors are digitized onboard the satellite at a rate of 39,936 samples per second per channel. Each sample step corresponds to an angle of scanner rotation of 0.95 milliradians. At this sampling rate, there are 1.362 samples per instantaneous field of view (IFOV). A total of 2,048 samples is obtained per channel per Earth scan, which spans an angle of +/-55.4 degrees from nadir.

4.1.1 Collection Environment

The NOAA satellites orbit Earth at an altitude of 833 km. From this space platform, the data are transmitted to a ground receiving station.

4.1.2 Source/Platform

Launch and available dates for the TIROS-N series of satellites from CCRS are:

```
Satellite    Launch Date         Date Range
---------    -----------    -------------------------
TIROS-N      13-Oct-1978    19-Oct-1978 to 30-Jan-1980
NOAA-6       27-Jun-1979    21-Aug-1984 to 23-Jan-1986
NOAA-B       29-May-1980    Failed to achieve orbit
NOAA-7       23-Jun-1981    24-Jul-1983 to 30-Dec-1984
NOAA-8       28-Mar-1983    24-Jul-1983 to 13-Aug-1985
NOAA-9       12-Dec-1984    16-Sep-1985 to 19-Mar-1995
NOAA-10      17-Sep-1986    11-Oct-1986 to 15-Nov-1993
NOAA-11      24-Sep-1988    28-Jun-1989 to 13-Sep-1994
NOAA-12      14-May-1991    11-Aug-1993 to present
NOAA-14      30-Dec-1994    15-May-1995 to present
```

4.1.3 Source/Platform Mission Objectives

The AVHRR is designed for multispectral analysis of meteorologic, oceanographic, and hydrologic parameters. The objective of the instrument is to provide radiance data for investigation of clouds, land water boundaries, snow and ice extent, ice or snow melt inception, day and night cloud distribution, temperatures of radiating surfaces, and SST. It is an integral member of the payload on

the advanced TIROS-N spacecraft and its successors in the NOAA series, and as such contributes data required to meet a number of operational and research-oriented meteorological objectives.

4.1.4 Key Variables
Emitted radiation and reflected radiation.

4.1.5 Principles of Operation
The AVHRR is a four- or five-channel scanning radiometer that detects emitted and reflected radiation from Earth in the visible, near-infrared, middle-infrared, and thermal-infrared regions of the electromagnetic spectrum. A fifth channel was added to the follow-on instrument designated AVHRR/2 and flown on NOAA-7, -9, -11, and -14 to improve the correction for atmospheric water vapor.

4.1.6 Sensor/Instrument Measurement Geometry
The AVHRR is a cross-track scanning system. The IFOV of each sensor is approximately 1.4 milliradians, giving a spatial resolution of 1.1 km at the satellite subpoint. There is about a 36 percent overlap between IFOVs (1.362 samples per IFOV). The scanning rate of the AVHRR is six scans per second, and each scan spans an angle of +/-55.4 degrees from the nadir.

4.1.7 Manufacturer of Sensor/Instrument
ITT Aerospace

4.2 Calibration
No in-flight visible channel calibration is performed.

4.2.1 Specifications

```
IFOV                1.4 mrad
RESOLUTION          1.1 km
ALTITUDE            833 km
SCAN RATE           360 scans/min (1.362 samples per IFOV)
SCAN RANGE          -55.4 to 55.4 degrees
SAMPLES/SCAN        2,048 samples per channel per Earth scan
```

4.2.1.1 Tolerance
A signal-to-noise ratio of 3:1 at 0.5-percent albedo.

4.2.2 Frequency of Calibration
The Naval Research Laboratory's (NRL's) TIROS-N calibration overlay performs the calibration on blocks of telemetry data. For LAC/HRPT acquisitions, a block consists of 20 scan lines. Calibration begins by reading the calibration parameters into memory. For each scan line of telemetry in a block, the following process takes place:
- Telemetry data are extracted and unpacked.
- Ramp calibration data for each of the five channels are decommutated.

4.2.3 Other Calibration Information
None given.

5. Data Acquisition Methods

The BOREAS level-4c AVHRR-LAC images were acquired through the CCRS. Some radiometric and geometric corrections are applied to produce the imagery in a spatially corrected form (Lambert Conformal Conic (LCC) projection). A full level-4c AVHRR-LAC image contains approximately 1,200 pixels in each of approximately 1,200 lines. Before any geometric corrections, the ground resolution ranges from 1.1 km at nadir to 2.5 km x 6.8 km at the scanning extremes. Each pixel value is stored in a 2-byte field starting with level-4b products. The level-4c images were processed through software developed at CCRS. The raw data are available from the CCRS PASS.

6. Observations

6.1 Data Notes
None.

6.2 Field Notes
None.

7. Data Description

7.1 Spatial Characteristics

7.1.1 Spatial Coverage
The spatial characteristics for these LAI and FPAR images are the same as for the BOREAS level-4c AVHRR-LAC imagery, which covers the entire 1,000-km by 1,000-km BOREAS region. This contains the Northern Study Area (NSA), the Southern Study Area (SSA), and the transect region between the SSA and NSA.

The North American Datum of 1983 (NAD83) coordinates for the corners of the LAI and FPAR images are:

```
                          Latitude        Longitude
                          ----------      -----------
Northwest  (1,1)          59.36395°N      115.40859°W
Northeast  (1,1200)       61.01294°N       93.28553°W
Southwest  (1200,1)       48.83387°N      110.25229°W
Southeast  (1200,1200)    50.02993°N       93.73857°W
```

The northwest corner has a distance (1109.76 km west, 7900.04 km north) from the origin (95°W and 0°N) of the LCC coordinate. The pixel size is exactly 1 km.

```
The NAD83 corner coordinates of the BOREAS region are:


            Latitude     Longitude
            --------     ---------
Northwest   59.979°N     111.000°W
Northeast   58.844°N      93.502°W
Southwest   51.000°N     111.000°W
Southeast   50.089°N      96.970°W
```

```
The NAD83 corner coordinates of the SSA are:

                Latitude        Longitude
                --------        ---------
Northwest       54.319°N        106.227°W
Northeast       54.223°N        104.236°W
Southwest       53.513°N        106.320°W
Southeast       53.419°N        104.368°W


The NAD83 corner coordinates of the NSA are:

                Latitude        Longitude
                --------        ---------
Northwest       56.249°N         98.824°W
Northeast       56.083°N         97.241°W
Southwest       55.542°N         99.045°W
Southeast       55.379°N         97.489°W
```

7.1.2 Spatial Coverage Map
Not available.

7.1.3 Spatial Resolution
Before any geometric corrections, the spatial resolution varies from 1.1 km at nadir to approximately 2.5 x 6.8 km at the extreme edges of the scan. The level-4b composite AVHRR-LAC images have had geometric corrections applied so that the pixel size is 1 km in all bands. Only pixels with view zenith angles 57 degrees or less are used in level-4c product. The LAI and FPAR images have the same 1.0-km spatial resolution.

7.1.4 Projection
The coordinate system is the LCC with the two standard parallels at 49 degrees north and 77 degrees north, respectively, and the meridian at 95 degrees west.

7.1.5 Grid Description
The LAI and FPAR images are the same as the level-4 images, which are projected into the LCC projection described in Section 7.1.4 at a resolution of 1.0 km per pixel (grid cell) in both the X and Y directions.

7.2 Temporal Characteristics

7.2.1 Temporal Coverage
The overall time period of AVHRR data acquisition in 1994 was from 09-Apr through 10-Sep. Ten-day composite images of NDVI for this period were produced at level-4c. Three NDVI composite images corresponding to the IFC periods were used for LAI and FPAR calculation (see Section 7.2.2).

7.2.2 Temporal Coverage Map
The 1994 compositing periods from the level-4c data set used for the LAI and FPAR parameter images were the following 10-day periods, one during each IFC:

May 21-31
July 21-31
September 1-10

7.2.3 Temporal Resolution
The daily images are composited into nominally cloud-free images over 10-day periods. One 10-day compositing period was selected to represent each 1994 IFC to create the three LAI and FPAR images for this data set.

7.3 Data Characteristics

7.3.1 Parameter/Variable
LAI
FPAR
7.3.2 Variable Description/Definition
LAI is defined as one half the total leaf area per unit ground surface area. For four-sided spruce needles, two sides are included. To derive LAI from the digital numbers (DN) in the image, use the following formula:

$$LAI = (DN-1)/10$$

Green FPAR is the fraction of incident PAR that is absorbed by the green leaves in the canopy. It excludes the fraction reflected back to space and the fraction absorbed by the background (moss, soil and understory in forest, and soil in the crops), but it includes the small fraction that is reflected by the background and absorbed by the green leaves on the way back to space. To derive FPAR from the DNs in the image, use the following formula:

$$FPAR = (DN-1)/100$$

7.3.3 Unit of Measurement
Both LAI and FPAR are unitless; for LAI, it can be expressed as m^2 of leaf area/m^2 of ground surface area.

7.3.4 Data Source
The level-4c AVHRR data used to create this product was processed and provided by the CCRS.

7.3.5 Data Range
Both the LAI and FPAR images are 8-bit images; i.e., the DNs vary from 0 to 255.

7.4 Sample Data Record
Not applicable to image data.

8. Data Organization

8.1 Data Granularity
The smallest unit of data tracked by the BOREAS Information System (BORIS) is the entire set of AVHRR parameter image files, the readme file, and the coordinate conversion code.

8.2 Data Format(s)

8.2.1 Uncompressed Data Files

This data product consists of the following data files:

```
                                    logical
file          description       record size
------    ----------------------    -----------
  1       Header/Readme                 80
  2       FPAR_AVHRR_IFC1_94.IMG      1200
  3       FPAR_AVHRR_IFC2_94.IMG      1200
  4       FPAR_AVHRR_IFC3_94.IMG      1200
  5       LAI_AVHRR_IFC1_94.IMG       1200
  6       LAI_AVHRR_IFC2_94.IMG       1200
  7       LAI_AVHRR_IFC3_94.IMG       1200
  8       lcc_1200.f                    80
```

The header file contains descriptive information about the files in the product.

Each of the composite images contain 1,200 8-bit (1-byte) pixels in each of the 1,200 lines. The image file format is the same as that of any band sequential (BSQ) image file.

The FORTRAN program, "lcc_1200.f", is provided for the calculation of longitude and latitude for any given pixel and line in the image. When using the software, you need to input the pixel and line numbers relative to the top-left pixel, which is (1,1). A version of the lcc_1200 code written in C is available on request from Jing M. Chen at CCRS.

8.2.2 Compressed CD-ROM Files

On the BOREAS CD-ROMs, the ASCII header file for this image is stored as ASCII text; however, the image files have been compressed with the Gzip (GNU zip) compression program (file_name.gz). These data have been compressed using gzip version 1.2.4 and the high compression (-9) option (Copyright (C) 1992-1993 Jean-loup Gailly). Gzip uses the Lempel-Ziv algorithm (Welch, 1994) also used in the zip and PKZIP programs. The compressed files may be uncompressed using gzip (with the -d option) or gunzip. Gzip is available from many Web sites (for example, the ftp site prep.ai.mit.edu/pub/gnu/gzip-*.*) for a variety of operating systems in both executable and source code form. Versions of the decompression software for various systems are included on the CD-ROMs.

9. Data Manipulations

9.1 Formulae

9.1.1 Derivation Techniques and Algorithms

9.1.1.1 LAI Maps

The NDVI was first converted to the simple ratio (SR) using

$$SR = (1+NDVI)/(1-NDVI)$$

In the calculation of LAI from SR, different algorithms were used for the following 10 land cover types: water, mixed wood, deciduous, conifer, transitional forest, tundra, barren lands, cropland, rangeland/pasture, and built-up areas. For water, barren lands, and built-up areas, LAI is set to zero. An algorithm for the cropland is formulated using available NDVI-LAI relationships in the literature (Holben et al., 1980; Gardner and Blad, 1986; Aase et al., 1986; Wiegand et al., 1992; Li et al., 1993). The algorithm for boreal conifer forests is derived from our recent work (Chen and Cihlar, 1996). The methodology for ground truth LAI measurements is described in Chen and Cihlar (1995a and 1995b) and Chen (1996a). The algorithm for deciduous forests is also based on our own work,

but is less accurate because of the vegetation dynamics and insufficient field data for the seasonal coverage. Mixed wood and transitional forests are considered as the intermediate case between conifer and deciduous forests. Tundra and rangeland/pasture are treated the same as cropland because of lack of data. Summer images are less useful for determining the overstory NDVI in conifer canopies because of the understory effect (Chen and Cihlar, 1996); therefore, the IFC-2 and IFC-3 LAI values for conifer species were taken to be 1.12 and 1.05 times the IFC-1 values. A ceiling of LAI values was used for each IFC to remove 'speckles' (unreasonably large LAI values caused by noise in NDVI data). These ceilings were 5.5, 6.0, and 5.7 for IFC-1, IFC-2, and IFC-3, respectively.

The algorithms for boreal forests were developed by correlating SR from Landsat-5 Thematic Mapper (TM) with ground-based LAI measurements. In the application of the algorithm to AVHRR images, a factor of 1.10 was used to increase the NDVI of AVHRR to account for sensor differences.

Caution should be taken when using these LAI values for the calculation of FPAR because some models only use LAI inputs, while FPAR is calculated from LAI. Because of the canopy architectural difference between the species, it is suggested that the LAI values should be reduced by 50% for conifers, 25% for deciduous and mixed wood, and 10% for agricultural crops and tundra in the calculation of radiation interception using Beer's Law.

The equations used in the LAI algorithm are:

```
IFC-1 and IFC-3:
LAI=0.594(SR-2.781)        For mixed wood
LAI=0.475(SR-2.781)        For deciduous forest
LAI=0.792(SR-2.781)        For transitional forest
LAI=1.188(SR-2.781)        For conifer forest
LAI=0.325(SR-1.5)          For tundra
LAI=0.325(SR-1.5)          For cropland
LAI=0.325(SR-1.5)          For rangeland and pasture
LAI=0                      For water, barren, and built-up areas


IFC-2:
LAI=0.493(SR-3.637)        For mixed wood
LAI=0.394(SR-3.637)        For deciduous forest
LAI=0.657(SR-3.637)        For transitional forest
LAI=1.12*LAI in IFC-1      For conifer forest
LAI=0.325(SR-1.5)          For tundra
LAI=0.325(SR-1.5)          For cropland
LAI=0.325(SR-1.5)          For rangeland and pasture
LAI=0                      For water, barren, and built-up areas
```

As shown above, the background SR values are all the same because of the lack of field data. The background values were obtained through regression for the conifer species. The IFC-2 LAI values were calculated from IFC-1 values to minimize the background effect (Chen and Cihlar, 1996).

9.1.1.2 Daily Green FPAR Maps
Green FPAR refers to the fraction absorbed by green leaves only after the removal of the contribution of the supporting woody material to the PAR absorption. The instantaneous green FPAR is integrated over the day with a weight equal to the cosine of the solar zenith angle to obtain the daily green FPAR presented in the map. The daily green FPAR can be used as a parameter to convert the daily absorbed PAR to daily total incident PAR. The dates for IFC-1, IFC-2, and IFC-3 are the same as those for LAI maps.

Similar to the calculation of LAI, different algorithms for the daily green FPAR were used for the 10 land cover types. FPAR for water, barren lands, and built-up areas is assumed to be zero. An algorithm for the cropland is formulated using measurements from crop fields (Chen, unpublished). The algorithm is similar to that of Asrar et al. (1984). The algorithms for boreal conifer forests are published in Chen (1996b). For deciduous cover, the algorithm is formulated using eight sites in the

midsummer (Chen, unpublished). The algorithms are linear relationships between SR and FPAR. Tundra and rangeland/pasture are treated the same as cropland because of lack of data.

The values for boreal forests within the map are the most reliable. FPAR of the overstory is calculated from the downwelling and upwelling PAR measurements at two levels: above and below the canopy, for over 30 stands. The below-canopy measurements were made using the Tracing Radiation and Architecture of Canopies (TRAC) instrument (BOREAS RSS-07 Ground Measurements of LAI and FPAR). Because the downwelling PAR through the overstory and upwelling PAR reflected from the forest floor are highly variable, average values were obtained from closely spaced measurements over long transects (50-340 m). Simultaneous measurements of the downwelling and upwelling PAR above the forests were made on micrometeorological towers established for BOREAS. The data were collected at the beginning, middle, and end of the growing season to consider the effect of seasonal vegetation dynamics and the change in solar zenith angle (Chen, 1996b).

The equations used in the FPAR algorithm are:

IFC-1 and IFC-3:

```
FPAR=0.170(SR-2.044)      For mixed wood
FPAR=0.147(SR-2.044)      For deciduous forest
FPAR=0.176(SR-2.044)      For transitional forest
FPAR=0.221(SR-2.044)      For conifer forest
FPAR=0.138(SR-1.5)        For tundra
FPAR=0.138(SR-1.5)        For cropland
FPAR=0.138(SR-1.5)        For rangeland and pasture
FPAR=0                    For water, barren, and built-up areas
```

IFC-1 and IFC-3:

```
FPAR=0.147(SR-3.074)      For mixed wood
FPAR=0.127(SR-3.074)      For deciduous forest
FPAR=0.154(SR-3.074)      For transitional forest
FPAR=1.05*FPAR in IFC-1   For conifer forest
FPAR=0.138(SR-1.5)        For tundra
FPAR=0.138(SR-1.5)        For cropland
FPAR=0.138(SR-1.5)        For rangeland and pasture
FPAR=0                    For water, barren, and built-up areas
```

In the equations the background SR changes between IFCs. The background values are different from the LAI equations because the SR-FPAR relationship is not strictly linear. These values were found from the regressions for the conifer species. A refinement of the algorithm would be to use the Modified SR (MSR, Chen 1996c), which is more linearly related to FPAR. IFC-2 LAI values for conifers are directly related to IFC-1 values because the background effect in IFC-1 is smaller (Chen and Cihlar, 1996). This assumes the normal seasonal growth situation.

Because of lack of complete field data for all cover types, the most reliable data are for conifer, transitional forest, and cropland. The images with quality quote 04 (on a scale of 05) will be made available upon request. Please notify the contacts listed in Section 2.3 regarding any problems you encounter.

9.2 Data Processing Sequence

The processing steps from NDVI to LAI and FPAR are summarized above (Section 9.1); the processing steps leading to NDVI are described in the document for BOREAS level-4c AVHRR-LAC images. The relevant descriptions are copied below for convenience.

The level-4c processing sequence is called Atmosphere, Bidirectional and Contamination Corrections of CCRS (ABC3) and is described in more detail by Cihlar et al. (1997a, 1997b).

9.2.1 Processing Steps

Step 1: Top-of-the-Atmosphere (TOA) reflectance
   TOA reflectance for channel 1 or 2 is calculated from the corrected TOA radiance, L*(new), with the formula given by Teillet (1992). Values of gain G and offset O were calculated with consideration of postlaunch sensor degradation (Teillet and Holben, 1994).

Step 2: Atmospheric correction of AVHRR channels 1 and 2
   The algorithm Simplified Method for Atmospheric Correction (SMAC) (Rahman and Dedieu, 1994) was used in the processing. The processing was carried out assuming a water content of 2.3 g/cm^2 and ozone content of 0.319 cm-atm. A constant value of 0.05 was used for optical depth at 550 nm. The corrections were computed on a pixel basis using solar zenith, view zenith, and relative azimuth channels.

Step 3: Identification of contaminated pixels
   A new procedure was developed to identify the 'contaminated' pixels; i.e., pixels where the surface vegetation or soil signal is obscured (Cihlar, 1996). The procedure, dubbed Cloud Elimination from Composites using Albedo and NDVI Trend (CECANT), is based on the high sensitivity of NDVI to the presence of clouds, aerosol, and snow. Three features of the annual surface reflectance trend are used: the high contrast between the albedo (represented by AVHRR channel 1) of land, especially when fully covered by green vegetation, and clouds or snow/ice; the average NDVI value (expected value for that pixel and compositing period); and the monotonic trend in NDVI. Four thresholds are required in CECANT to identify a partially contaminated pixel (i,j,t) where i and j are pixel coordinates and t is the compositing period:

C1(t):	The maximum channel 1 reflectance of a clear-sky, snow- or ice-free land pixel in the data set.
Rmin(t):	The maximum acceptable deviation of the measured value NDVI(i,j,t) below the estimated NDVIa(i,j,t).
Rmax(t):	The maximum acceptable deviation of the measured value NDVI(i,j,t) above the estimated NDVIa(i,j,t).
Zmax(t):	The maximum acceptable deviation of the measured value NDVI(i,j,t) above the estimated NDVImax(i,j,t).

   NDVImax(i,j,t) and NDVIa(i,j,t) were calculated using the Fourier-Adjustment, Solar Zenith Angle Corrected, Interpolated, Reconstructed (FASIR) model of Sellers et al. (1994), which approximates the seasonal NDVI curve with a third-order Fourier transform. Before the computation, missing NDVI values between first and last measurements were replaced through linear interpolation after finding the seasonal peak for each pixel, using the rationale and algorithm of Cihlar and Howarth (1994). A constant value of 0.30 was used for C1. The upper and lower limits for R and Z were determined separately for each composite period using R and Z histograms (Cihlar, 1996). Using these thresholds, a cloud mask was prepared for each composite period.

Step 4: Corrections for bidirectional reflectance effects in channels 1 and 2
   The model of Roujean et al. (1992) as modified by Wu et al. (1995) was used to characterize the seasonal bidirectional reflectance function for each cover type. Land cover-dependent model coefficients were derived (Li et al., 1995) using a map of Canada with pixel size of 1 km prepared with AVHRR data (Pokrant, 1991). Only cloud-free pixels were included in the derivation of the model coefficients, and no bidirectional corrections for snow- or ice-covered areas were made. The resulting models were used to compute channel 1 and 2 reflectance for view zenith of 0 degrees and solar zenith of 45 degrees.

Step 5: Replacement of contaminated pixels for AVHRR channels 1 and 2
     Two cases were recognized: pixels contaminated either during or at the end of the growing season. For pixels contaminated during the growing season, the new values were found through linear interpolation for both channels 1 and 2. At the end of the growing season, it was assumed that the annual trajectory for individual channels as well as for NDVI could be approximated by a second-degree polynomial. The polynomial was fitted to the plot of corrected reflectance for all clear-sky periods, starting with the first clear-sky composite period after 01-Aug. After the best-fit coefficients were determined, the new values were calculated using the polynomial coefficients to replace contaminated pixels in each channel prior to the first clear pixel or after the last such pixel.

Step 6: NDVI processing
     Because of imperfections in the bidirectional corrections of channels 1 and 2, the NDVI values computed from atmospherically corrected NDVI were also retained. However, corrections for solar zenith angle were desirable in view of the known dependence of the NDVI on the solar zenith angle. The coefficients of Sellers et al. (1994) were used for the various land cover classes. The new set of NDVI values was then computed for a reference solar zenith angle of 45 degrees based on the equations of Sellers et al. (1994). The NDVI values for the missing or contaminated pixels were interpolated as in Step 5 above.

Step 7: Compression
     BORIS staff copied the ASCII and compressed the binary files for release on CD-ROM.

9.2.2 Processing Changes
     None.

9.3 Calculations
     See Section 9.2.1.

9.3.1 Special Corrections/Adjustments
     See Section 9.2.1.

9.3.2 Calculated Variables
     See Section 9.2.1.

9.4 Graphs and Plots
     None.

10. Errors

10.1 Sources of Error
     The sources of errors in LAI and FPAR are: (1) ground measurements, (2) use of algorithms based on Landsat TM that include image geometric and radiometric corrections and atmospheric correction, (3) error in determining the response difference between TM and AVHRR sensors, (4) the error associated with the AVHRR NDVI product.
     The major sources of error in AVHRR NDVI are due to the inaccurate knowledge of atmospheric conditions during image acquisition (and thus the use of nominal values for atmospheric corrections) and imperfect modeling of the bidirectional effects.

10.2 Quality Assessment

10.2.1 Data Validation by Source
     None given.

10.2.2 Confidence Level/Accuracy Judgment

The FPAR images are more accurate than the LAI images. The relative error in LAI is estimated to be 20% for conifers and transitional forests; 25% for deciduous and mixed covers; and 30% for cropland, grassland, and tundra. The relative error in daily green FPAR is estimated to be less than 10% for all cover types.

10.2.3 Measurement Error for Parameters

See Section 10.2.2.

10.2.4 Additional Quality Assessments

None given.

10.2.5 Data Verification by Data Center

BORIS staff displayed the LAI and FPAR images as a visual check that the images were what was expected.

11. Notes

11.1 Limitations of the Data

The calculated LAI and FPAR maps should be considered the best estimate for this moderate resolution. The distribution patterns and the magnitude of LAI and FPAR values for each cover type are indeed very reasonable. The resampling scheme used for the original channel images makes the actual resolution coarser than 1 km. It is on the order of 2-3 km in reality (Cihlar et al., 1997b). Subpixel water bodies and mixture of different cover types in a pixel can incur errors in the calculated results. Lack of data makes the calculations for rangeland, tundra, and mixed wood types least reliable.

11.2 Known Problems with the Data

None.

11.3 Usage Guidance

Before uncompressing the Gzip files on CD-ROM, be sure that you have enough disk space to hold the uncompressed data files. Then use the appropriate decompression program provided on the CD-ROM for your specific system.

11.4 Other Relevant Information

None.

12. Application of the Data Set

None given.

13. Future Modifications and Plans

None given.

14. Software

14.1 Software Description
A Fortran program, "lcc_1200.f", is provided for the calculation of longitude and latitude for any given pixel and line in the image. When using the software, you need to input the pixel and line numbers relative to the top-left pixel, which is (1,1). Gzip (GNU zip) uses the Lempel-Ziv algorithm (Welch, 1994) used in the zip and PKZIP commands.

14.2 Software Access
A version of the lcc_1200 code written in C is available on request from contacts listed in Section 2.3. Gzip is available from many Web sites across the Internet (for example, FTP site prep.ai.mit.edu/pub/gnu/gzip-*.*) for a variety of operating systems in both executable and source code form. Versions of the decompression software for various systems are included on the CD-ROMs.

15. Data Access

The RSS-07 regional LAI and FPAR images are available from the Earth Observing System Data and Information System (EOSDIS) Oak Ridge National Laboratory (ORNL) Distributed Active Archive Center (DAAC).

15.1 Contact Information
For BOREAS data and documentation please contact:

ORNL DAAC User Services
Oak Ridge National Laboratory
P.O. Box 2008 MS-6407
Oak Ridge, TN 37831-6407
Phone: (423) 241-3952
Fax: (423) 574-4665
E-mail: ornldaac@ornl.gov or ornl@eos.nasa.gov

15.2 Data Center Identification
Earth Observing System Data and Information System (EOSDIS) Oak Ridge National Laboratory (ORNL) Distributed Active Archive Center (DAAC) for Biogeochemical Dynamics http://www-eosdis.ornl.gov/.

15.3 Procedures for Obtaining Data
Users may obtain data directly through the ORNL DAAC online search and order system [http://www-eosdis.ornl.gov/] and the anonymous FTP site [ftp://www-eosdis.ornl.gov/data/] or by contacting User Services by electronic mail, telephone, fax, letter, or personal visit using the contact information in Section 15.1.

15.4 Data Center Status/Plans
The ORNL DAAC is the primary source for BOREAS field measurement, image, GIS, and hardcopy data products. The BOREAS CD-ROM and data referenced or listed in inventories on the CD-ROM are available from the ORNL DAAC.

16. Output Products and Availability

16.1 Tape Products
The data can be made available on 8-mm or Digital Archive Tape (DAT) media.

16.2 Film Products
None.

16.3 Other Products
These data are available on the BOREAS CD-ROM series.

17. References

17.1 Platform/Sensor/Instrument/Data Processing Documentation

Buffam, A. 1994. GEOCOMP User Manual. Internal Report, Canada Centre for Remote Sensing, Ottawa, Ontario.

Cihlar, J. 1996. Identification of contaminated pixels in AVHRR composite images for studies of land biosphere. Remote Sensing of Environment 56:149-163.

Cihlar, J. and J. Howarth. 1994. Detection and removal of cloud contamination from AVHRR composite images. IEEE Transactions on Geoscience and Remote Sensing 32: 427-437.

Cihlar, J., H. Ly, Z. Li, J. Chen, H. Pokrant, and F. Huang. 1997a. Multitemporal, multichannel data sets for land biosphere studies: artifacts and corrections. Remote Sensing of Environment 60:35-57.

Cihlar, J., J. Chen, and Z. Li. 1997b. Seasonal AVHRR multichannel data sets and products for studies of surface-atmosphere interactions. Journal of Geophysical Research 102(D24):29,625-29,640.

Kidwell, K. 1991. NOAA Polar Orbiter Data User's Guide, NCDC/SDSD. (Updated from original 1984 edition.)

Li, Z., J. Cihlar, X. Zheng, L. Moreau, and H. Ly. 1996. The bidirectional effects of AVHRR measurements over northern regions. IEEE Transactions on Geoscience and Remote Sensing (accepted).

Pokrant, H. 1991. Land cover map of Canada derived from AVHRR images. Manitoba Remote Sensing Centre, Winnipeg, Manitoba, Canada.

Rahman, H. and G. Dedieu. 1994. SMAC: a simplified method for the atmospheric correction of satellite measurements in the solar spectrum. International Journal for Remote Sensing 15: 123-143.

Robertson, B., A. Erickson, J. Friedel, B. Guindon, T. Fisher, R. Brown, P. Teillet, M. D'Iorio, J. Cihlar, and A. Sancz. 1992. GEOCOMP, a NOAA AVHRR geocoding and compositing system. Proceedings of the ISPRS Conference, Commission 2, Washington, DC: 223-228.

Roujean, J.-L., M. Leroy, and P.-Y. Deschamps. 1992. A bidirectional reflectance model of the Earth's surface for the correction of remote sensing data. Journal of Geophysical Research 97(D18): 20,455-20,468.

Salisbury, J.W. and D.M. D'Aria. 1992. Emissivity of terrestrial materials in the 8-1 m atmospheric window. Remote Sensing of Environment 42: 83-106.

Sellers, P.J., S.O. Los, C.J. Tucker, C.O. Justice, D.A. Dazlich, G.A. Collatz, and D.A. Randall, 1994. A global 1o by 1 o NDVI data set for climate studies. Part 2: The generation of global fields of terrestrial biophysical parameters from the NDVI. International Journal of Remote Sensing.

Sobrino, J.A., C. Coll, and V. Caselles. 1991. Atmospheric correction for land surface temperature using NOAA-11 AVHRR channels 4 and 5. Remote Sensing of Environment 38: 19-34.

Suttles, J.T., R.N. Green, P. Minnis, G.L. Smith, W.F. Staylor, B.A. Wielicki, I.J. Walker, D.F. Young, V.R. Taylor, and L.L. Stowe. 1989 Angular radiation models for Earth-atmosphere system, Vol. 1, Shortwave radiation, NASA Ref. Publ., 1184, 84 pp.

Teillet, P.M. 1992. An algorithm for the radiometric and atmospheric correction of AVHRR data in the solar reflective channels. Remote Sensing of Environment 41: 185-195.

Teillet, P.M. and B.N. Holben. 1994. Towards operational radiometric calibration of NOAA AVHRR imagery in the visible and near-infrared channels. Canadian Journal of Remote Sensing 20: 1-10.

Townshend, J. (Ed.). 1995. Global data sets for the land from AVHRR. International Journal of Remote Sensing 15: 3315-3639 (special issue describing several program generating composite AVHRR image data sets).

Van de Griend, A.A. and M. Owe. 1993. On the relationship between thermal emissivity and the normalized difference vegetation index for natural surfaces. International Journal of Remote Sensing 14(6): 1119-1131.

Welch, T.A. 1984. A Technique for High Performance Data Compression. IEEE Computer, Vol. 17, No. 6, pp. 8-19.

Wiegand, C.L., S.J. Maas, J.K. Aase, J.L. Hatfield, P.J. Pinter, Jr., R.D. Jackson, E.T. Kanemasu, and R.L. Lapitan. 1992. Multisite Analyses of Spectral-Biophysical Data for Wheat. Remote Sensing of Environment 42: 1-21.

Wu, A., Z. Li, and J. Cihlar. 1995. Effects of land cover type and greenness on AVHRR bidirectional reflectances: Analysis and removal J. Geophy. Res. (in press).

17.2 Journal Articles and Study Reports

Aase, J.K., J.P. Millard, and B.S. Brown. 1986. Spectral Radiance Estimates of Leaf Area and Leaf Phytomass of Small Grains and Native Vegetation. IEEE Transactions on Geoscience and Remote Sensing 24: 685-692.

Asrar, G., M. Fuchs, E.T. Kanemasu, and J.H. Hatfield. 1984. Estimating absorbed photosynthetic radiation and leaf area index from spectral reflectance in wheat. Agron. J. 76:300-306.

Becker, F. and Z.L. Li. 1990. Towards a local split window method over land surface. International Journal of Remote Sensing 3: 369-393.

Chen, J.M. 1996a. Optically-based methods for measuring seasonal variation of leaf area index in boreal conifer stands. Agric. For. Meteorology 80:135-163.

Chen, J.M. 1996b. Canopy Architecture and remote sensing of the fraction of photosynthetically active radiation absorbed by boreal forests. IEEE Trans. Geosci Remote Sens. 34:1353-1368.

Chen, J.M. 1996c. Evaluation of vegetation indices and a modified simple ratio for boreal applications. Can. J. Remote Sens. 22:229-242.

Chen, J.M. and J. Cihlar. 1995a. Plant canopy gap size analysis theory for improving optical measurements of leaf area index of plant canopies. Applied Optics 34:6211-6222.

Chen, J.M. and J. Cihlar. 1995b. Quantifying the effect of canopy architecture on optical measurements of leaf area index using two gap size analysis methods. IEEE Trans. Geosci. Remote Sens. 33:777-787.

Chen, J.M. and J. Cihlar 1996. Retrieving leaf area index in boreal forests using Landsat TM images. Remote Sensing of Environment 55:153-162.

Cihlar, J. and P.M. Teillet. 1995. Forward piecewise linear calibration model for quasi-real time processing of AVHRR data. Canadian Journal of Remote Sensing 21: 22-27.

Coll, C., V. Caselles, J.A. Sobrino, and E. Valor. 1994. On the atmospheric dependence of the split-window equation for land surface temperature. International Journal for Remote Sensing 15(1): 105-122.

Gardner, B.R., and B.L. Blad. 1986. Evaluation of Spectral Reflectance Models To Estimate Corn Leaf Area While Minimizing the Influence of Soil Background Effects. Remote Sensing of Environment 20: 183-193.

Holben, B.N., C.J. Tucker, and C-J. Fan. 1980. Spectral Assessment of Soybean Leaf Area and Leaf Biomass. Photogrammetric Engineering and Remote Sensing 46: 651-656.

Li Z, T.H. Demetriadesshah, E.T. Kanemasu, J.K. Shultis, and M.B. Kirkham. 1993. Use Of 2nd Derivatives Of Canopy Reflectance For Monitoring Prairie Vegetation Over Different Soil Backgrounds. Remote Sensing Of Environment 44: (1) 81-87 APR 1993.

Newcomer, J., D. Landis, S. Conrad, S. Curd, K. Huemmrich, D. Knapp, A. Morrell, J. Nickeson, A. Papagno, D. Rinker, R. Strub, T. Twine, F. Hall, and P. Sellers, eds. 2000. Collected Data of The Boreal Ecosystem-Atmosphere Study. NASA. CD-ROM.

Sellers, P. and F. Hall. 1994. Boreal Ecosystem-Atmosphere Study: Experiment Plan. Version 1994-3.0, NASA BOREAS Report (EXPLAN 94).

Sellers, P. and F. Hall. 1996. Boreal Ecosystem-Atmosphere Study: Experiment Plan. Version 1996-2.0, NASA BOREAS Report (EXPLAN 96).

Sellers, P., F. Hall, and K.F. Huemmrich. 1996. Boreal Ecosystem-Atmosphere Study: 1994 Operations. NASA BOREAS Report (OPS DOC 94).

Sellers, P., F. Hall, and K.F. Huemmrich. 1997. Boreal Ecosystem-Atmosphere Study: 1996 Operations. NASA BOREAS Report (OPS DOC 96).

Sellers, P., F. Hall, H. Margolis, B. Kelly, D. Baldocchi, G. den Hartog, J. Cihlar, M.G. Ryan, B. Goodison, P. Crill, K.J. Ranson, D. Lettenmaier, and D.E. Wickland. 1995. The boreal ecosystem-atmosphere study (BOREAS): an overview and early results from the 1994 field year. Bulletin of the American Meteorological Society. 76(9):1549-1577.

Sellers, P.J., F.G. Hall, R.D. Kelly, A. Black, D. Baldocchi, J. Berry, M. Ryan, K.J. Ranson, P.M. Crill, D.P. Lettenmaier, H. Margolis, J. Cihlar, J. Newcomer, D. Fitzjarrald, P.G. Jarvis, S.T. Gower, D. Halliwell, D. Williams, B. Goodison, D.E. Wickland, and F.E. Guertin. 1997. BOREAS in 1997: Experiment Overview, Scientific Results and Future Directions. Journal of Geophysical Research 102(D24): 28,731-28,770.

17.3 Archive/DBMS Usage Documentation
None.

18. Glossary of Terms

None given.

19. List of Acronyms

```
ABC3     - Atmosphere, Bidirectional and Contamination Corrections of CCRS
AEAC     - Albers Equal-Area Conic
APT      - Automatic Picture Transmission
ASCII    - American Standard Code for Information Interchange
AVHRR    - Advanced Very High Resolution Radiometer
BOREAS   - BOReal Ecosystem-Atmosphere Study
BORIS    - BOREAS Information System
BPI      - Bytes Per Inch
BSQ      - Band Sequential
CCRS     - Canada Centre for Remote Sensing
CCT      - Computer-Compatible Tape
CD-ROM   - Compact Disk-Read-Only Memory
CECANT   - Cloud Elimination from Composite Using Albedo and NDVI Trend
DAAC     - Distributed Active Archive Center
DAT      - Digital Archive Tape
DN       - Digital Number
EOS      - Earth Observing System
EOSDIS   - EOS Data and Information System
EROS     - Earth Resources Observation System
FASIR    - Fourier-Adjustment, Solar Zenith Angle corrected, Interpolated,
           Reconstructed
FPAR     - Fraction of PAR absorbed by plant canopies
GAC      - Global Area Coverage
GEOCOMP  - Geocoding and Compositing System
GIS      - Geographic Information System
GSFC     - Goddard Space Flight Center
HRPT     - High-Resolution Picture Transmission
IFC      - Intensive Field Campaign
IFOV     - Instantaneous Field-of-View
ISLSCP   - International Satellite Land Surface Climatology Project
LAC      - Local Area Coverage
LAI      - Leaf Area Index
LCC      - Lambert Conformal Conic
MRSC     - Manitoba Remote Sensing Centre
MSR      - Modified SR
NAD83    - North American Datum of 1983
NASA     - National Aeronautics and Space Administration
```

```
NDVI    - Normalized Difference Vegetation Index
NEdT    - Noise Equivalent Differential Temperature
NOAA    - National Oceanic and Atmospheric Administration
NRL     - Naval Research Laboratory
NSA     - Northern Study Area
ORNL    - Oak Ridge National Laboratory
PAR     - Photosynthetically Active Radiation
PASS    - Prince Albert Satellite Station
PRT     - Platinum Resistor Thermometer
RSS     - Remote Sensing Science
SMAC    - Simplified Method for Atmospheric Correction
SR      - Simple Ratio
SSA     - Southern Study Area
SST     - Sea Surface Temperature
TIROS   - Television and Infrared Observation Satellite
TM      - Thematic Mapper
TOA     - Top-of-the-Atmosphere
TRAC    - Tracing Radiation and Architecture of Canopies (a LAI and FPAR
          optical instrument)
URL     - Uniform Resource Locator
```

20. Document Information

20.1 Document Revision Date
Written: 25-Sep-1997
Last Updated: 26-Jul-1999
20.2 Document Review Date(s)
BORIS Review: 06-Oct-97
Science Review: 10-Jan-98

20.3 Document ID

20.4 Citation
When using these data, please include the following acknowledgment as well as citations of relevant papers in Section 17.2:

The AVHRR-LAC level-4c composite images resulted from a joint effort between BOREAS staff at CCRS and NASA GSFC. The original data were acquired by CCRS and processed as level-3b products by the MRSC in Winnipeg, Manitoba. The present level-4c product was created by CCRS staff using a method developed at CCRS. The respective contributions of the above individuals and agencies to completing this data set are greatly appreciated.

If using data from the BOREAS CD-ROM series, also reference the data as:

Chen, J.M. and J. Cihlar, "Retrieval of Boreal Forest Leaf Area Index From Multiple Scale Remotely Sensed Vegetation Indices." In Collected Data of The Boreal Ecosystem-Atmosphere Study. Eds. J. Newcomer, D. Landis, S. Conrad, S. Curd, K. Huemmrich, D. Knapp, A. Morrell, J. Nickeson, A. Papagno, D. Rinker, R. Strub, T. Twine, F. Hall, and P. Sellers. CD-ROM. NASA, 2000.

Also, cite the BOREAS CD-ROM set as:

Newcomer, J., D. Landis, S. Conrad, S. Curd, K. Huemmrich, D. Knapp, A. Morrell, J. Nickeson, A. Papagno, D. Rinker, R. Strub, T. Twine, F. Hall, and P. Sellers, eds. Collected Data of The Boreal Ecosystem-Atmosphere Study. NASA. CD-ROM. NASA, 2000.

20.5 Document Curator

20.6 Document URL

REPORT DOCUMENTATION PAGE

1. AGENCY USE ONLY *(Leave blank)*

2. REPORT DATE
August 2000

3. REPORT TYPE AND DATES COVERED
Technical Memorandum

4. TITLE AND SUBTITLE
Technical Report Series on the Boreal Ecosystem-Atmosphere Study (BOREAS)
BOREAS RSS-7 Regional LAI and FPAR Images From 10-Day
AVHRR-LAC Composites

5. FUNDING NUMBERS
923
RTOP: 923-462-33-01

6. AUTHOR(S)
Jing Chen and Josef Cihlar
Forrest G. Hall and Jaime Nickeson, Editors

7. PERFORMING ORGANIZATION NAME(S) AND ADDRESS (ES)
Goddard Space Flight Center
Greenbelt, Maryland 20771

8. PEFORMING ORGANIZATION REPORT NUMBER
2000-03136-0

9. SPONSORING / MONITORING AGENCY NAME(S) AND ADDRESS (ES)
National Aeronautics and Space Administration
Washington, DC 20546-0001

10. SPONSORING / MONITORING AGENCY REPORT NUMBER
TM—2000–209891
Vol. 52

11. SUPPLEMENTARY NOTES
J. Chen and J. Cihlar: Canada Centre for Remote Sensing; Jaime Nickeson: Raytheon ITSS

12a. DISTRIBUTION / AVAILABILITY STATEMENT
Unclassified–Unlimited
Subject Category: 43
Report available from the NASA Center for AeroSpace Information,
7121 Standard Drive, Hanover, MD 21076-1320. (301) 621-0390.

12b. DISTRIBUTION CODE

13. ABSTRACT *(Maximum 200 words)*

The BOREAS RSS-7 team collected various data sets to develop and validate an algorithm to allow the retrieval of the spatial distribution of LAI from remotely sensed images. AVHRR level-4c 10-day composite NDVI images produced at CCRS were used to produce images of LAI and the FPAR absorbed by plant canopies for the three summer IFCs in 1994 across the BOREAS region. The algorithms were developed based on ground measurements and Landsat TM images (Chen and Cihlar, 1996; Chen, 1996b). The data are stored in binary image format files.

14. SUBJECT TERMS
BOREAS, remote sensing science, LAI, FPAR.

15. NUMBER OF PAGES
21

16. PRICE CODE

17. SECURITY CLASSIFICATION OF REPORT
Unclassified

18. SECURITY CLASSIFICATION OF THIS PAGE
Unclassified

19. SECURITY CLASSIFICATION OF ABSTRACT
Unclassified

20. LIMITATION OF ABSTRACT
UL